

RESEARCH ARTICLE

First-principles study of electronic structure and magnetic properties of $\text{SrTi}_{1-x}\text{M}_x\text{O}_3$ (M = Cr, Mn, Fe, Co, or Ni)

Xin-Long Dong^{1,2}, Kun-Hua Zhang^{3,*}, Ming-Xiang Xu^{2,†}

¹College of Physics and Information Engineering, Shanxi Normal University, Linfen 041004, China

²Department of Physics and Key Laboratory of MEMS of the Ministry of Education, Southeast University, Nanjing 210096, China

³ICQD, Hefei National Laboratory for Physical Sciences at Microscale, University of Science and Technology of China, Hefei 230026, China

Corresponding authors. E-mail: *zhangkh1@ustc.edu.cn, †mxxu@seu.edu.cn

Received April 6, 2018; accepted May 29, 2018

We used first-principles calculations to conduct a comparative study of the structure and the electronic and magnetic properties of SrTiO_3 doped with a transition metal (TM), namely, Cr, Mn, Fe, Co, or Ni. The calculated formation energies indicate that compared with Sr, Ti can be substituted more easily by the TM ions. The band structures show that $\text{SrTi}_{0.875}\text{Cr}_{0.125}\text{O}_3$ and $\text{SrTi}_{0.875}\text{Co}_{0.125}\text{O}_3$ are half metals, $\text{SrTi}_{0.875}\text{Fe}_{0.125}\text{O}_3$ is a metal, and $\text{SrTi}_{0.875}\text{Mn}_{0.125}\text{O}_3$ is a semiconductor. The 3d TM-doped SrTiO_3 exhibits various magnetic properties, ranging from ferromagnetism (Cr-, Fe-, and Co-doped SrTiO_3) to antiferromagnetism (Mn-doped SrTiO_3) and nonmagnetism (Ni-doped SrTiO_3). The total magnetic moments are $4.0\mu_B$, $6.23\mu_B$, and $2.0\mu_B$ for $\text{SrTi}_{0.75}\text{Cr}_{0.25}\text{O}_3$, $\text{SrTi}_{0.75}\text{Fe}_{0.25}\text{O}_3$, and $\text{SrTi}_{0.75}\text{Co}_{0.25}\text{O}_3$, respectively. Room-temperature ferromagnetism can be expected in Cr-, Fe-, and Co-doped SrTiO_3 , which agrees with the experimental observations. The electronic structure calculations show that the spin polarizations of the 3d states of the TM atoms are responsible for the ferromagnetism in these compounds. The magnetism of TM-doped SrTiO_3 is explained by the hybridization between the TM-3d states and the O-2p states.

Keywords first-principles calculations, SrTiO_3 , electronic structure, ferromagnetism

PACS numbers 71.15.Mb, 75.47.Lx, 73.50.-h

1 Introduction

Perovskite oxides containing transition metal (TM) ions are known to exhibit ferroelectric polarization, colossal magneto-resistance, and high dielectric constants; hence, they have great potential for use in oxide-based electronic devices [1–6]. Moreover, impurity doping may profoundly affect the electronic structure, magnetism, and ferroelectricity of SrTiO_3 [7, 8]. Hase *et al.* [9] performed a systematic *ab initio* calculation of the electronic structure of $\text{Sr}_{1-x-y}\text{La}_{x+y}\text{Ti}_{1-x}\text{Cr}_x\text{O}_3$ by changing the doping concentrations x and y as $0 < x < 0.2$ and $-0.2 < y < 0.2$; they found that the total magnetic moment was almost proportional to the Cr concentration, whereas it was more strongly proportional to the La concentration. Meanwhile, within the framework of the local spin-density approximation, Nakayama and Katayama-

Yoshida [10] performed *ab initio* calculations for BaTiO_3 doped with a 3d TM (from Sc to Cu); their results indicated that BaTiO_3 doped with Mn, Cr, or Fe would be a promising candidate for ferromagnetism.

Recently, many experimental studies have reported ferromagnetism in 3d TM-doped SrTiO_3 . For example, Lee *et al.* [11] reported that Co–Mn co-doped single-crystal SrTiO_3 produced ferromagnetic (FM) behavior over a broad range of TM concentrations, indicating prominently the possibility of intrinsic ferromagnetism with high Curie temperature and large magnetization. Furthermore, Zhang *et al.* [12] prepared Mn and La co-doped SrTiO_3 -based thin films and observed FM behavior at room temperature, most likely due to the magnetic coupling between the induced free electrons and Mn 3d spins. Kim also grew $\text{SrTi}_{1-x}\text{Fe}_x\text{O}_3$ ($x \leq 0.5$) films on (001) LaAlO_3 substrates, and their structural and magnetic studies indicated that the ferromagnetism

was intrinsic [13]. Conversely, $\text{SrTi}_{1-x}\text{Fe}_x\text{O}_3$ films deposited in an oxygen atmosphere possess no ferromagnetism at room temperature [14]. Meanwhile, several studies have observed room-temperature ferromagnetism (RTFM) in $\text{SrTi}_{1-x}\text{Co}_x\text{O}_3$ [15–17]. However, the theoretical knowledge about the magnetic properties of 3d transition-metal-doped SrTiO_3 is limited. The magnetic properties and the corresponding interaction mechanism of 3d TM-doped SrTiO_3 are still not fully understood.

2 Computational method

All calculations were performed with the framework of density functional theory as implemented in the Vienna *ab initio* simulation package [18, 19]. The electron-core interaction was described by the projected augmented wave [20, 21] pseudopotential with the general gradient approximation (GGA) parameterized by Perdew, Burke, and Ernzerhof (PBE) [22]. The electron wave function was expanded in plane waves up to a cutoff energy of 450 eV, and a $5 \times 5 \times 5$ Monkhorst–Pack k-grid [23] was used to sample the Brillouin zone of the supercell. The convergence criterion for the electronic energy was set to 10^{-5} eV. The Hellman–Feynman force was smaller than 0.01 eV/Å in the optimized structure. To treat the effective on-site Coulomb interaction U and exchange interaction J , we also used the GGA + U method to better describe the localized TM d electrons.

3 Results and discussion

In our calculations, we used a 40-atom $2 \times 2 \times 2$ supercell, as shown in Fig. 1, in which one Ti atom is replaced by one TM atom, corresponding to a doping concentration of 12.5%. The crystal structure of SrTiO_3 is cubic perovskite with a space group of $Pm\bar{3}m$, and a lattice constant of 3.905 Å at room temperature. Figure 1 shows the structure of 3d TM-doped (Cr, Mn, Fe, Co, or Ni) SrTiO_3 , where the green, gray, blue, and red balls denote the Sr, Ti, TM, and O atoms, respectively. The lattice constant of the cubic SrTiO_3 structure is 3.941 Å, which agrees with that reported by earlier studies [24, 25]. The calculated lattice constants are 3.930 , 3.927 , 3.935 , 3.923 , and 3.924 Å for Cr-, Mn-, Fe-, Co-, and Ni-doped SrTiO_3 , respectively. The calculated TM–O bond lengths are 1.934 , 1.928 , 1.951 , 1.926 , and 1.927 Å for Cr–O, Mn–O, Fe–O, Co–O, and Ni–O, respectively, indicating a slight contraction in comparison to the original Ti–O bond length (1.970 Å). This and the slight decrease in the lattice constant are due to the radius of the TM atom being smaller than that of the Ti atom.

To evaluate the relative stability of TM-doped SrTiO_3 ,

we calculated the formation energy E_f as

$$E_f = E_{doped} - E_{pure} + E_x - E_{TM}, \quad (1)$$

where E_{doped} and E_{pure} are the total energies of the $2 \times 2 \times 2$ SrTiO_3 supercell with and without TM doping, respectively; E_x is the energy of a Ti or Sr ion; E_{TM} is the energy of the TM ion. As shown in Fig. 2, the calculated results indicate that the TM atoms prefer to substitute Ti rather than Sr. Furthermore, Cr-, Mn-, or Fe-doped SrTiO_3 may be easier to realize experimentally compared with Co- or Ni-doped SrTiO_3 .

To understand the electronic structure and magnetic properties of $\text{SrTi}_{1-x}\text{TM}_x\text{O}_3$, we calculated its band structure, total density of states (TDOS), and partial density of states (PDOS). Figures 3, 4, and 5 show the spin-resolved band structures, TDOS, and PDOS, respectively, of SrTiO_3 and $\text{SrTi}_{0.875}\text{TM}_{0.125}\text{O}_3$. As shown in Figs. 3(a₁) and (a₂), SrTiO_3 is an indirect bandgap insulator with the top of its valence band at the R point

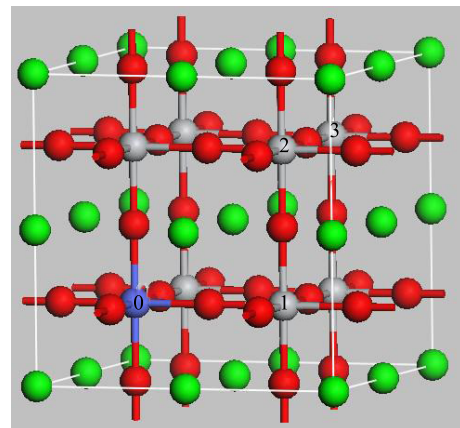


Fig. 1 Supercell used in the calculations. Green, gray, blue, and red balls indicate Sr, Ti, transition metal (TM), and O atoms, respectively. The positions of Ti atoms substituted by TM atoms are denoted by 0–3.

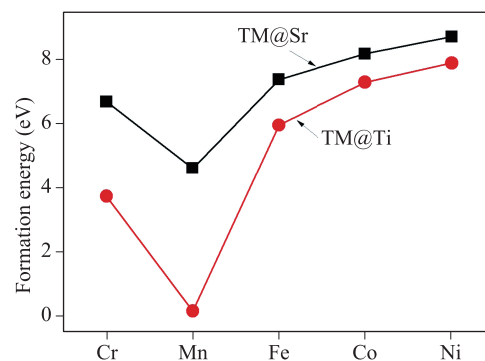


Fig. 2 Formation energies for metal-doped SrTiO_3 structures.

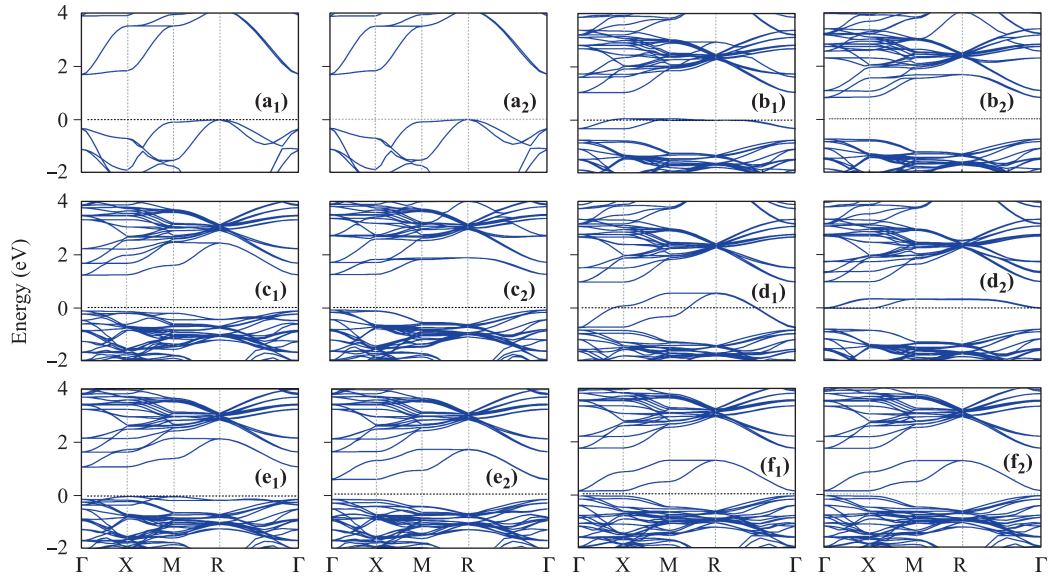


Fig. 3 Band structures of SrTiO₃ and SrTi_{0.875}M_{0.125}O₃ (M = Cr, Mn, Fe, Co, or Ni). (**a**₁–**f**₁) represent the majority spin channel; (**a**₂–**f**₂) represent the minority spin channel. The Fermi level is set to zero.

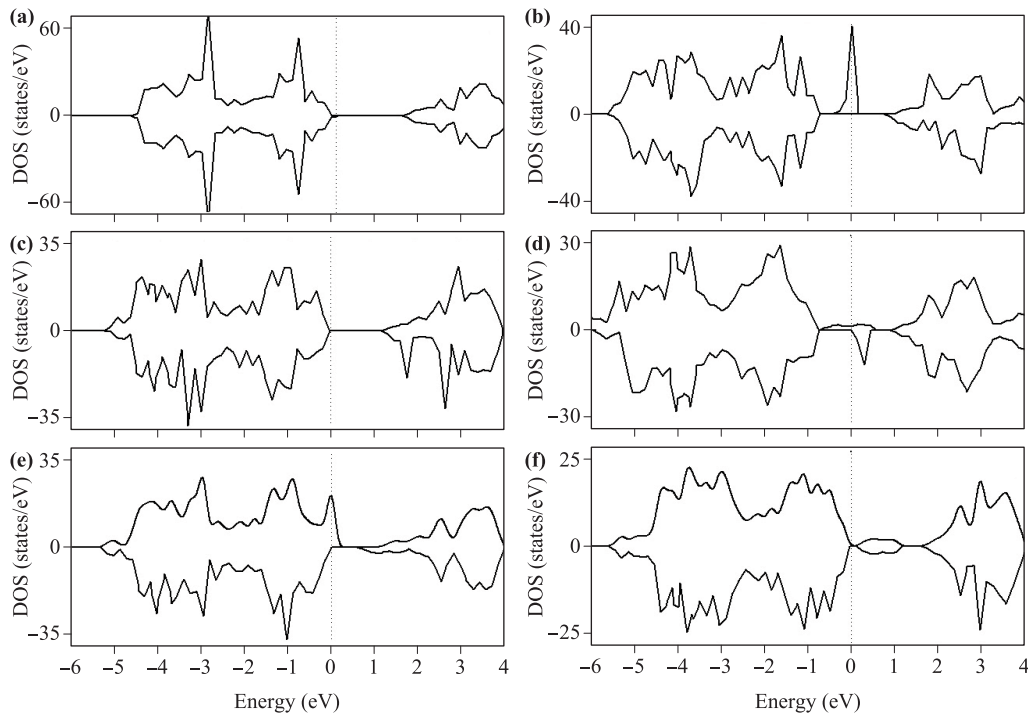


Fig. 4 Total DOS for (a) pure SrTiO₃, (b) Cr-, (c) Mn-, (d) Fe-, (e) Co-, and (f) Ni-doped SrTiO₃ respectively. The Fermi level is set to zero and indicated by the vertical dashed line.

and the bottom of its conduction band at the Γ point. The calculated bandgap of pure SrTiO₃ is 1.80 eV, close to the value of 1.78 eV calculated by Zhang *et al.* [26], which is much smaller than the experimental value due to the well-known shortcomings of the GGA calculations. In our research, we neglected the bandgap error

between different systems because our focus is to determine the manner in which the energy levels of a given system change. As shown in Fig. 6, the bandgaps of TM-doped SrTiO₃ differ significantly from that of SrTiO₃. The calculated bandgaps are 0.75, 1.15, 0.445, 0.44, and 0.45 eV for Cr-, Mn-, Fe-, Co-, and Ni-doped SrTiO₃, re-

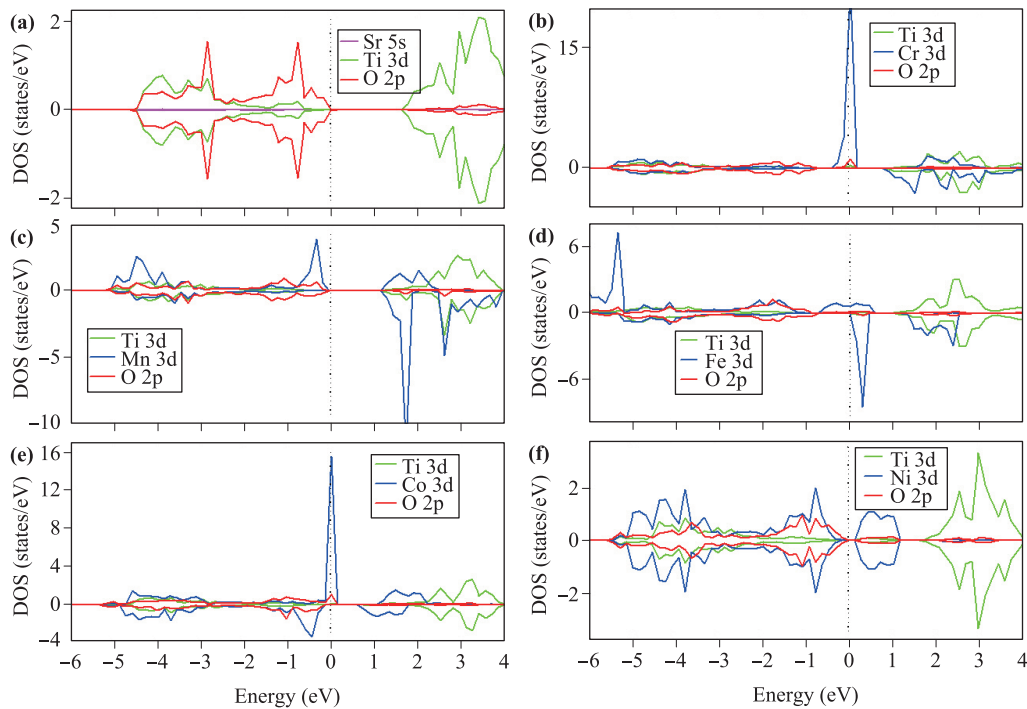


Fig. 5 PDOS for (a) pure SrTiO₃, (b) Cr-, (c) Mn-, (d) Fe-, (e) Co-, and (f) Ni-doped SrTiO₃ respectively. The Fermi level is set to zero and indicated by the vertical dashed line.

spectively. The Mn- and Ni-doped SrTiO₃ have smaller bandgaps than that of SrTiO₃, which agrees with the calculations of Yang *et al.* [27].

Figure 3 shows that pure SrTiO₃ and Ni-doped SrTiO₃ are nonmagnetic. For Cr-, Mn-, Fe-, and Co-doped SrTiO₃, the spin-up and spin-down states are asymmetrical near the Fermi level, implying that these systems should be magnetic. Figure 4 shows that TM doping changes the density of states appreciably near the Fermi level and results in the spin polarization of the valence band and the conduction band. For Cr- or Fe-doped SrTiO₃, the TDOS peaks shift to lower energies and spin splitting is induced around the Fermi level. Consequently, Fe-doped SrTiO₃ is a magnetic metal, resulting from both the ma-

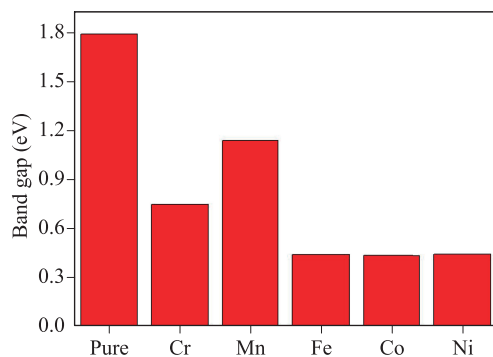


Fig. 6 Bandgaps for metal-doped SrTiO₃ structures.

jority and minority spin states crossing the Fermi level. For Cr- and Co-doped SrTiO₃, the majority spin band crosses the Fermi level, whereas the minority spin band possess a bandgap around the Fermi level. Therefore, Cr- and Co-doped SrTiO₃ are half-metals with 100% spin polarization, for which applications in spintronics are possible. The PDOS of the TM-doped SrTiO₃ are shown in Fig. 5, where it is shown that the spin splitting of Cr-, Mn-, Fe-, and Co-doped SrTiO₃ originate from the O-2p and TM-3d states. The peak across the Fermi level is primarily due to the TM-3d state, with some contribution from the 2p-O state but little from the Ti-3d state. Consequently, the localized states near the Fermi level are primarily due to the 2p-O and TM-3d valence electrons. This hybridization of the TM-3d and O-2p states is critical in the induced magnetic moments.

Next, we investigated the magnetic properties of 3d TM-doped SrTiO₃. In Table 1, we noticed that Cr-, Mn-, Fe-, and Co-doped SrTiO₃ favor spin-polarized states; their total energies are 570, 1572.6, 741.5, and 30.5 meV, respectively, which are lower than those of non-spin-polarized states. To determine the magnetic ground state, we systematically investigate the substitution of two doped atoms for two Ti atoms in the 40-atom supercell, corresponding to a dopant concentration of 25%. In Fig. 1, the replaced Ti atoms are marked with numbers 0–3. Three possible structures are obtained by replacing two Cr, Mn, Fe, or Co for the two Ti positions

Table 1 Optimized lattice constants, X-O (X = Cr, Mn, Fe, Co, or Ni) bond lengths. Total energy difference $\Delta E = E_{nsp} - E_{sp}$ between non-spin-polarized (E_{nsp}) and spin-polarized (E_{sp}) states.

Models	a (Å)	X-O (Å)	ΔE (meV)
SrTiO ₃	3.941	1.970	/
SrTi _{0.875} Cr _{0.125} O ₃	3.930	1.934	570
SrTi _{0.875} Mn _{0.125} O ₃	3.927	1.928	1577.9
SrTi _{0.875} Fe _{0.125} O ₃	3.935	1.951	741.5
SrTi _{0.875} Co _{0.125} O ₃	3.923	1.926	30.5
SrTi _{0.875} Ni _{0.125} O ₃	3.924	1.927	0

at (0, 1), (0, 2), and (0, 3), respectively. To determine the magnetic stability of the doped systems, we performed spin-polarized calculations for the parallel and the antiparallel arrangement of spins of the TM atoms. Table 2 lists the energy difference between the FM and antiferromagnetic (AFM) states ($\Delta E_{FM} = E_{AFM} - E_{FM}$), the relative ground-state energy of the FM state (E_{FM}), the TM-TM distance, and the total magnetic moment of the TM-TM pair in the ground state for each configuration. We used the magnetization energy ($\Delta E_{FM} = E_{AFM} - E_{FM}$) to indicate the stability of the FM state; a positive value indicates that the FM state is more stable than the AFM state. According to our calculated results, the ΔE_{FM} values of Cr-, Fe-, and Co-doped SrTiO₃ are all positive, indicating that the FM state is the ground state. The calculated magnetic moments are $4.00\mu_B$, $6.23\mu_B$, and $2.0\mu_B$ for two Cr-, Fe-, and Co-doped SrTiO₃ supercells, respectively. For the Cr-doped SrTiO₃, the total magnetic moment ($4.0\mu_B$) arises pri-

marily from the Cr atoms ($1.85\mu_B$ per Cr atom); for the Fe-doped SrTiO₃, the total magnetic moment ($6.23\mu_B$) arises primarily from the Fe atoms ($2.61\mu_B$ per Fe atom); for the Co-doped SrTiO₃, the total magnetic moment ($2.0\mu_B$) arises primarily from the Co atoms ($0.72\mu_B$ per Co atom).

For the Mn-doped SrTiO₃, the AFM state is more stable than the FM state, indicating that RTFM should not be expected in the Mn-doped SrTiO₃. However, for the Cr-doped SrTiO₃, the FM state is 218.8 meV lower than that of the AFM state; therefore, RTFM should be expected in the Cr-doped SrTiO₃. In addition, for the Fe-doped SrTiO₃, the energy of the FM state is 161 meV lower than that of the corresponding AFM state; such a large difference between the FM and AFM states implies that RTFM should be expected. The results agree with those of recent experimental research on Fe-doped SrTiO₃ [13]. For the Co-doped SrTiO₃, the energy of a state with FM coupling is 92.4 meV lower than that of the corresponding state with AFM coupling, which agrees with previous experimental observations of RTFM [16, 17].

Finally, to verify how the on-site Coulomb interactions with TM d electrons affect the magnetic properties, we used GGA + U ($U = 3.1$ eV) calculations to study the FM stability of Cr-, Mn-, Fe-, and Co-doped SrTiO₃. The results are listed in Table 3. We found that the magnetic interactions between two Cr, Fe, and Co atoms are still FM coupling; the energy of the FM state is 48.1, 162.6, and 113.97 meV lower, respectively, than that of the AFM state. Meanwhile, for the Mn-doped SrTiO₃, the energy of the FM state is 15.1 meV higher than that of the AFM state, which agrees with the GGA-calculated result.

Table 2 Summary of X-X distance (d_{X-X}), relative ground-state energy of ferromagnetic (FM) state (E_{FM}), relative energy between FM and antiferromagnetic (AFM) states ($\Delta E = E_{AFM} - E_{FM}$), average magnetic moment of X atom (M_X), and magnetic coupling for each (0, i) structure of the two-X-atom-doped SrTiO₃ with GGA method.

Type	(0, i)	d_{X-X} (Å)	E_{FM} (meV)	ΔE (meV)	M_{total} (μ_B)	M_X (μ_B)	Coupling
SrTi _{0.75} Cr _{0.25} O ₃	(0, 1)	3.905	0	218.9	4.00	1.85	FM
	(0, 2)	5.523	52.8	38.7	4.00	1.85	FM
	(0, 3)	6.764	165.9	4.3	4.00	1.83	FM
SrTi _{0.75} Mn _{0.25} O ₃	(0, 1)	3.905	289.5	-121.7	6.02	2.64	AFM
	(0, 2)	5.523	23.9	-45.7	6.00	2.625	AFM
	(0, 3)	6.764	0	-0.15	6.00	2.62	AFM
SrTi _{0.75} Fe _{0.25} O ₃	(0, 1)	3.905	0	161.25	6.23	2.61	FM
	(0, 2)	5.523	354	108.2	4.14	1.76	FM
	(0, 3)	6.764	436.7	5.4	5.41	2.8	FM
SrTi _{0.75} Co _{0.25} O ₃	(0, 1)	3.905	10.1	341.5	3.20	1.25	FM
	(0, 2)	5.523	0	92.4	2.00	0.72	FM
	(0, 3)	6.764	123.5	9.2	2.00	0.72	FM

Table 3 Summary of energy of FM state (E_{FM}), energy of AFM state (E_{AFM}), relative energy between FM and AFM states ($\Delta E = E_{AFM} - E_{FM}$), average magnetic moment of X atom (M_X), and magnetic coupling for each $(0, i)$ structure of two-X-atom-doped SrTiO₃ with GGA + U method.

Type	$(0, i)$	E_{FM}	E_{AFM}	ΔE (meV)	M_X (μ_B)	Coupling
SrTi _{0.75} Cr _{0.25} O ₃	(0, 1)	-292.331902	-292.326542	5.36	2.11	FM
	(0, 2)	-292.268703	-291.348247	92.04	2.11	FM
	(0, 3)	-292.376126	-292.328027	48.1	2.10	FM
SrTi _{0.75} Mn _{0.25} O ₃	(0, 1)	-291.288062	-291.304171	-16.1	3.1	AFM
	(0, 2)	-291.453931	-291.469071	-15.1	2.97	AFM
	(0, 3)	-291.446864	-291.447067	-0.2	2.97	AFM
SrTi _{0.75} Fe _{0.25} O ₃	(0, 1)	-287.228523	-287.065862	162.6	3.67	FM
	(0, 2)	-285.895420	-287.009795	-1114.3	3.29	AFM
	(0, 3)	-286.484204	-286.368232	115.97	3.83	FM
SrTi _{0.75} Co _{0.25} O ₃	(0, 1)	-281.184157	-281.070183	113.97	2.58	FM
	(0, 2)	-280.971116	-280.898991	72.125	1.08	FM
	(0, 3)	-281.130980	-280.617253	513.7	1.05	FM

4 Conclusions

We investigated the electronic structure and the magnetic properties of 3d TM-doped SrTiO₃ using first-principles calculations. The density of states shows that SrTi_{0.875}Cr_{0.125}O₃ and SrTi_{0.875}Co_{0.125}O₃ are half-metals, SrTi_{0.875}Fe_{0.125}O₃ is a metal, and SrTi_{0.875}Mn_{0.125}O₃ is a semiconductor. Our results show that RTFM can be predicted in SrTi_{0.75}Cr_{0.25}O₃, SrTi_{0.75}Fe_{0.25}O₃, and SrTi_{0.75}Co_{0.25}O₃.

Acknowledgements This work was supported by the National Natural Science Foundation of China (Grant No. 11747124).

References

1. D. D. Cuong, B. Lee, K. M. Choi, H. S. Ahn, S. Han, and J. Lee, Oxygen vacancy clustering and electron localization in oxygen-deficient SrTiO₃: LDA + U study, *Phys. Rev. Lett.* 98(11), 115503 (2007)
2. N. A. Pertsev, A. K. Tagantsev, and N. Setter, Phase transitions and strain-induced ferroelectricity in SrTiO₃ epitaxial thin films, *Phys. Rev. B* 61(2), R825 (2000)
3. J. H. Haeni, P. Irvin, W. Chang, R. Uecker, P. Reiche, Y. L. Li, S. Choudhury, W. Tian, M. E. Hawley, B. Craigo, A. K. Tagantsev, X. Q. Pan, S. K. Streiffer, L. Q. Chen, S. W. Kirchoefer, J. Levy, and D. G. Schlom, Room-temperature ferroelectricity in strained SrTiO₃, *Nature* 430(7001), 758 (2004)
4. M. D. Biegalski, Y. Jia, D. G. Schlom, S. Trolier-McKinstry, S. K. Streiffer, V. Sherman, R. Uecker, and P. Reiche, Relaxor ferroelectricity in strained epitaxial SrTiO₃ thin films on DyScO₃ substrates, *Appl. Phys. Lett.* 88(19), 192907 (2006)
5. H. M. Zhang, M. An, X. Y. Yao, and S. Dong, Orientation-dependent ferroelectricity of strained PbTiO₃ films, *Front. Phys.* 10(6), 107701 (2015)
6. R. N. Song, M. H. Hu, X. R. Chen, and J. D. Guo, Epitaxial growth and thermostability of cubic and hexagonal SrMnO₃ films on SrTiO₃(111), *Front. Phys.* 10(3), 106802 (2015)
7. A. Chen, Z. Yu, J. Scott, A. Loidl, R. Guo, A. S. Bhalla, and L. E. Cross, Dielectric polarization processes in Bi: SrTiO₃, *J. Phys. Chem. Solids* 61(2), 191 (2000)
8. M. Itoh, R. Wang, Y. Inaguma, T. Yamaguchi, Y. J. Shan, and T. Nakamura, Ferroelectricity induced by oxygen isotope exchange in strontium titanate perovskite, *Phys. Rev. Lett.* 82(17), 3540 (1999)
9. I. Hase, T. Saitoh, and T. Katsufuji, *Ab initio* calculation of charge- and spin-controlled Sr_{1-x-y}La_{x+y}Ti_{1-x}Cr_xO₃, *J. Magn. Magn. Mater.* 310(2), e281 (2007)
10. H. Nakayama and H. Katayama-Yoshida, Theoretical prediction of magnetic properties of Ba(Ti_{1-x}M_x)O₃ (M = Sc, V, Cr, Mn, Fe, Co, Ni, Cu), *Jpn. J. Appl. Phys.* 40(2), L1355 (2001)
11. J. S. Lee, Z. G. Khim, Y. D. Park, D. P. Norton, N. A. Theodoropoulou, A. F. Hebard, J. D. Budai, L. A. Boatner, S. J. Pearton, and R. G. Wilson, Magnetic properties of Co- and Mn-implanted BaTiO₃, SrTiO₃ and KTaO₃, *Solid-State Electron.* 47(12), 2225 (2003)
12. S. Y. Zhang, Y. H. Lin, C. W. Nan, R. Zhao, and J. He, Magnetic and electrical properties of (Mn, La)-codoped SrTiO₃ thin films, *J. Am. Ceram. Soc.* 91(10), 3263 (2008)

13. H. S. Kim, L. Bi, G. F. Dionne, and C. A. Ross, Magnetic and magneto-optical properties of Fe-doped SrTiO₃ films, *Appl. Phys. Lett.* 93(9), 092506 (2008)
14. D. H. Kim, N. M. Aimon, L. Bi, G. F. Dionne, and C. A. Ross, The role of deposition conditions on the structure and magnetic properties of SrTi_{1-x}Fe_xO₃ films, *J. Appl. Phys.* 111(7), 07A918 (2012)
15. Y. G. Zhao, S. R. Shinde, S. B. Ogale, J. Higgins, R. J. Choudhary, V. N. Kulkarni, R. L. Greene, T. Venkatesan, S. E. Lofland, C. Lanci, J. P. Buban, N. D. Browning, S. Das Sarma, and A. J. Millis, Co-doped La_{0.5}Sr_{0.5}TiO_{3-x}: Diluted magnetic oxide system with high Curie temperature, *Appl. Phys. Lett.* 83(11), 2199 (2003)
16. L. Bi, H. S. Kim, G. F. Dionne, and C. A. Ross, Structure, magnetic properties and magnetoelastic anisotropy in epitaxial Sr(Ti_{1-x}Co_x)O₃ films, *New J. Phys.* 12(4), 043044 (2010)
17. D. Yao, X. Zhou, and S. Ge, Raman scattering and room temperature ferromagnetism in Co-doped SrTiO₃ particles, *Appl. Surf. Sci.* 257(22), 9233 (2011)
18. G. Kresse and J. Hafner, *Ab initio* molecular dynamics for open-shell transition metals, *Phys. Rev. B* 48(17), 13115 (1993)
19. G. Kresse and J. Furthmuller, Efficiency of *ab-initio* total energy calculations for metals and semiconductors using a plane-wave basis set, *Comput. Mater. Sci.* 6(1), 15 (1996)
20. P. E. Blöchl, Projector augmented-wave method, *Phys. Rev. B* 50(24), 17953 (1994)
21. G. Kresse and D. Joubert, From ultrasoft pseudopotentials to the projector augmented-wave method, *Phys. Rev. B* 59(3), 1758 (1999)
22. J. P. Perdew, K. Burke, and M. Ernzerhof, Generalized gradient approximation made simple, *Phys. Rev. Lett.* 77(18), 3865 (1996)
23. H. J. Monkhorst and J. D. Pack, Special points for Brillouin-zone integrations, *Phys. Rev. B* 13(12), 5188 (1976)
24. Y. Zhang, J. Hu, E. Cao, L. Sun, and H. Qin, Vacancy induced magnetism in SrTiO₃, *J. Magn. Magn. Mater.* 324(10), 1770 (2012)
25. F. Li, K. Yu, L. L. Lou, Z. Su, and S. Liu, Theoretical and experimental study of La/Ni co-doped SrTiO₃ photocatalyst, *Mater. Sci. Eng. B* 172(2), 136 (2010)
26. C. Zhang, C. L. Wang, J. C. Li, K. Yang, Y. F. Zhang, and Q. Z. Wu, Substitutional position and insulator-to-metal transition in Nb-doped SrTiO₃, *Mater. Chem. Phys.* 107(2-3), 215 (2008)
27. C. Yang, T. Liu, Z. Cheng, H. Gan, and J. Chen, Study on Mn-doped SrTiO₃ with first principle calculation, *Physica B* 407(5), 844 (2012)